

Ion Exchange and Thermal Stability of MCM-41

Ji Man Kim, Ja Hun Kwak, Shinae Jun, and Ryong Ryoo*

Department of Chemistry and Center for Molecular Science, Korea Advanced Institute of Science and Technology, Taeduk Science Town, Taejeon, 305-701 Korea

Received: June 14, 1995; In Final Form: August 23, 1995[®]

Mesoporous molecular sieve MCM-41 with a Si/Al ratio of 39 was obtained by hydrothermal synthesis with a gel composition of 6 SiO₂:0.1 Al₂O₃:1 hexadecyltrimethylammonium chloride:0.25 dodecyltrimethylammonium bromide:0.25 tetrapropylammonium bromide:0.15 (NH₄)₂O:1.5 Na₂O:300 H₂O. The MCM-41 sample incorporating aluminum (AlMCM-41) was calcined in O₂ flow at 813 K and subsequently ion exchanged with Na⁺, K⁺, Ca²⁺, and Y³⁺. The ion exchange levels have been increased as high as 0.41 Na/Al, 0.36 K/Al, 0.37 Ca/Al and 0.39 Y/Al, respectively. Hydrothermal stability of the ion exchanged AlMCM-41 materials has been investigated with X-ray powder diffraction pattern, BET specific surface area, and magic-angle spinning ²⁷Al NMR spectroscopy, after the samples were heated for 2 h at various temperatures in O₂ flow saturated with water vapor at room temperature. The hydrothermal stability of the AlMCM-41 has been found to extend to the following temperatures depending on ion exchange: Y³⁺ (1170 K) ≈ Ca²⁺ > Na⁺ (1070 K) ≈ as calcined AlMCM-41 > pure-silica MCM-41 (980 K).

Introduction

In 1992, the discovery of a new family of mesoporous molecular sieves designated MCM-41 has been reported by researchers at the Mobil Corporation.^{1,2} The MCM-41 material possesses a uniform hexagonal array of linear channels constructed with a silica matrix like a honeycomb. The novelty in synthesis of the MCM-41 is the use of surfactant micelles, around which silicates polymerize hydrothermally to form the matrix structure. The surfactant can be removed by calcination at temperatures around 800 K. The channel diameter can be tailored within the range of 1.6–10 nm by the choice of the surfactant. Thus, the MCM-41 has dramatically extended the domain of the pore sizes of molecular sieves from the pore sizes of conventional zeolites (≤1.3 nm). Due to the large channel diameters, the MCM-41 materials attract much attention as a new host for large molecules as well as a new catalytic material.^{3–9}

Thermal stability is one of the most important physical properties to investigate for applications of MCM-41. Chen et al.¹⁰ reported that pure-silica MCM-41 could be heated to 1123 K in dry air or 1073 K in air with 8 Torr of water vapor before structural collapse began. However, the MCM-41 consisting of pure-silica framework is of limited use for applications as catalysts and adsorbents, due to lack of acid sites and ion exchange capacity. Aluminum can be incorporated within framework of the MCM-41 during synthesis, but studies^{11–13} using magic-angle spinning (MAS) ²⁷Al NMR spectroscopy show that the aluminum-containing MCM-41 (AlMCM-41) is readily dealuminated upon calcination. Corma et al.¹⁴ reported that calcined AlMCM-41 exhibited an acidity of medium strength comparable to that of a USY zeolite. However, it was not clear whether the acidity was due to Brønsted acidic protons that were ion exchanged to framework alumina sites for charge compensation as in zeolites or the acidity could be attributed to the formation of extraframework aluminum. Except that there was a report of copper ion exchange for the inclusion of a conducting polymer,^{6b} little was reported on ion exchange behavior of AlMCM-41 before the present work. Moreover,

there was no systematic report on thermal and hydrothermal stability of AlMCM-41.

Recent studies on the structure of MCM-41 have indicated that mesoporous channels were uniformly arranged like zeolite pores, but the channel wall seemed to have a local atomic structure similar to that of amorphous silica.¹⁰ From such a similarity of the MCM-41 wall to amorphous silica, ion exchange capacity of the AlMCM-41 may be assumed to be very small, compared with a crystalline aluminosilicate zeolite, e.g., ZSM-5, containing same amount of aluminum. Nevertheless, Wu and Bein^{6b} reported exchange of copper into AlMCM-41 for the synthesis of polyaniline inside the channel of the copper exchanged AlMCM-41. More recently, Ryoo and Kim¹⁵ have reported that the textural uniformity and thermal stability of MCM-41 were markedly improved by repeating pH adjustment to about 11 during hydrothermal reaction of sodium silicate and hexadecyltrimethylammonium (HTA) chloride. High-quality MCM-41 materials thus synthesized were calcined like conventional zeolites in air using a muffle furnace at 773 K, but the calcination caused no significant line broadening for the XRD pattern. The lattice contraction upon calcination was also negligible, contrary to large lattice contractions as much as 25% upon calcination in other studies.^{10,11} Furthermore, when yttrium was ion exchanged onto an AlMCM-41 sample synthesized likewise with repeating pH adjustment, the AlMCM-41 could be heated to 1173 K in O₂ flow with water vapor before structure collapsed seriously.

In the present investigation, we have extended our previous work on AlMCM-41 in order to clarify the ion exchange capacity of high-quality AlMCM-41 materials and dependence of the hydrothermal stability on the ion exchange. The ion exchanged AlMCM-41 has been investigated by ¹²⁹Xe NMR spectroscopy, in order to probe the presence of the ions inside the AlMCM-41 channel. The effect of the ion exchange on the hydrothermal stability has been investigated using XRD pattern, BET surface area, and MAS ²⁷Al NMR spectrum as a function of heating temperatures in O₂ flow with water vapor saturated at room temperature.

* To whom correspondence should be addressed.

[®] Abstract published in *Advance ACS Abstracts*, October 15, 1995.

Experimental Section

MCM-41 Synthesis Procedure. A pure-silica MCM-41 has been synthesized following a procedure of Ryoo and Kim.¹⁵ A clear solution of sodium silicate with a Na/Si ratio of 0.5 was prepared by combining 46.9 g of 1.00 M aqueous NaOH solution with 14.3 g of a colloidal silica, Ludox HS40 (39.5 wt % SiO₂, 0.4 wt % Na₂O, and 60.1 wt % H₂O, Du Pont) and heating the resulting gel mixture with stirring for 2 h at 353 K. The sodium silicate solution was dropwise added to a polypropylene bottle containing a mixture of 0.29 g of 28 wt % aqueous NH₃ solution and 20.0 g of 25 wt % HTAcl solution (Aldrich), with vigorous magnetical stirring at room temperature. The resulting gel mixture in the bottle had a molar composition of 6 SiO₂:1 HTAcl:1.5 Na₂O:0.15 (NH₄)₂O:250 H₂O. After stirring for 1 h more, the gel mixture was heated to 370 K for 1 day. The HTA-silicate mixture was then cooled to room temperature. Subsequently, pH of the reaction mixture was adjusted to 10.2 by dropwise addition of 30 wt % acetic acid with vigorous stirring. The reaction mixture after the pH adjustment was heated again to 370 K for 1 day. This procedure for pH adjustment to 10.2 and subsequent heating for 1 day was repeated twice more. The precipitated product, MCM-41 with HTA template, was filtered, washed with doubly distilled water, and dried in an oven at 370 K. The product was calcined in air under static conditions using a muffle furnace. The calcination temperature was increased from room temperature to 770 K over 10 h and maintained at 770 K for 4 h. The product yield was 90%, based on silica recovery.

For the synthesis of AlMCM-41, a surfactant source was obtained by dissolving 1.20 g of dodecyltrimethylammonium (DTA) bromide (Aldrich) and 1.04 g of tetrapropylammonium (TPA) bromide (Aldrich) in a mixture of 20.0 g of 25 wt % aqueous solution of HTAcl, 0.29 g of 28 wt % aqueous NH₃ solution, and 10.0 g of doubly distilled water. Alumina source was a solution of 0.43 g of sodium aluminate (Baker Analyzed Reagent) dissolved in 5.0 g of doubly distilled water. Silica source was 61.2 g of the same sodium silicate solution that was used for pure-silica MCM-41. The silicate solution was dropwise added to the surfactant source with vigorous stirring at room temperature. After the resulting surfactant-silicate gel mixture was stirred for 1 h at room temperature, the sodium aluminate solution was dropwise added with vigorous stirring. The resulting surfactant-aluminosilicate gel mixture had a molar composition of 6 SiO₂:0.1 Al₂O₃:1 HTAcl:0.25 DTABr:0.25 TPABr:0.15 (NH₄)₂O:1.5 Na₂O:300 H₂O. The gel mixture was stirred for 30 min more before heating in oven at 370 K for 1 day. The remainder of the synthesis procedure (i.e., heating and pH adjustment) except for the product washing and calcination was the same as for the above pure-silica MCM-41. After washing with doubly distilled water and drying at 370 K, the product was slurried in an ethanol-hydrochloric acid mixture (0.1 mol of HCl/L of ethanol) for 1 h under reflux conditions. Subsequently, the product was washed with ethanol at room temperature and dried at 370 K. Calcination of the product was carried out in O₂ flow (1 L g⁻¹ min⁻¹) while the sample was heated to 813 K over 10 h and maintained at this temperature for 10 h. Elemental analysis for the Si/Al ratio was performed with inductively coupled plasma (ICP) emission spectroscopy (Shimadzu, ICPS-1000III). The Si/Al ratio was 39. The product yield was 92%, considering the silica recovery. This sample with a Si/Al ratio of 39 was used for the characterization of ion exchange capacity and hydrothermal stability of AlMCM-41 in the present work.

Ion Exchange.¹⁶ Ion exchange of the AlMCM-41 was carried out with aqueous solutions of NaNO₃ (4.2 × 10⁻⁴ M),

KNO₃ (4.2 × 10⁻⁴ M), Ca(NO₃)₂·4H₂O (2.1 × 10⁻⁴ M), and Y(NO₃)₃·5H₂O (1.6 × 10⁻⁴ M). pH of the exchange solutions was between 6 and 7. For the ion exchange with Na⁺, 1.0 g of the as-calcined AlMCM-41 sample was slurried with 2.0 L of the NaNO₃ solution for 30 min at room temperature, using a magnetic stirrer. The molar ratio between the metal ion present in the solution and aluminum in the AlMCM-41 was 1.5. The AlMCM-41 sample, after the slurring was finished, was filtered and washed with doubly distilled water. This procedure for ion exchange is referred to a "slurry-filtration-wash" cycle. The cycle was repeated three times to increase the ion exchange level. The ion exchanged sample was dried in a drying oven at 370 K. The ion exchange with K⁺, Ca²⁺, and yttrium was carried out following the same procedure used for the Na⁺ ion exchange, except that the Na⁺ ion exchanged sample instead of the as-calcined sample was slurried with the other metal nitrate solutions. Elemental analysis of the ion exchanged samples using ICP gave the metal to Al ratios of 0.41 Na/Al, 0.36 K/Al, 0.37 Ca/Al, and 0.39 Y/Al.

Hydrothermal Treatments and Characterization. About 0.1 g of the calcined pure-silica MCM-41 and AlMCM-41 sample powder was uniformly spread over a fritted disk with 30 mm diameter inside a fused-silica flow reactor. Flows of dry O₂ and O₂ with 2.3 kPa of water vapor were passed downward through the sample bed at a rate of 2 L min⁻¹ per gram of sample, while the reactor was heated. The O₂ with water vapor was obtained by bubbling O₂ gas through a water bed at room temperature. The heating temperature was increased at a rate of 100 K h⁻¹ to a maximum temperature and maintained there for 2 h. The sample was characterized with XRD, BET surface area, and MAS ²⁷Al NMR after cooling to room temperature. The BET area measurement was carried out with N₂ adsorption using a volumetric gas adsorption apparatus. The MAS ²⁷Al NMR spectra were taken for both hydrated and dehydrated samples. The sample hydration was performed in an air chamber saturated with water using an aqueous solution saturated with NaCl at room temperature.

The XRD pattern was obtained with a Cu Kα X-ray source using a Rigaku D/MAX-III (3 kW) instrument. The MAS ²⁷Al NMR spectra were obtained at 296 K with a Bruker AM 300 instrument operating at 78.2 MHz. Relaxation delay for the ²⁷Al NMR was given as 2 s. The sample spinning rate was 3.5 kHz. For the ¹²⁹Xe NMR experiment, xenon gas (Matheson, 99.995%) was equilibrated over 30 min with the sample at 296 K under given pressure. ¹²⁹Xe NMR spectra were collected at 296 K with a Bruker AM 300 instrument operating at 83.0 MHz. The relaxation delay of 0.5 s was used to get the spectrum.

Results and Discussion

Quality of MCM-41 Depending on the Synthesis Procedures. XRD patterns of the MCM-41 samples synthesized in the present work are presented in Figure 1. The XRD patterns in Figure 1a,c consist of one very intense line, three weak lines, and one very weak line, which can be indexed to (100), (110), (200), (210), and (300) diffraction lines characteristic of a hexagonal structure of MCM-41, respectively.¹⁷ The unit cell dimension can be calculated by $a = 2d_{100}\sqrt{3}$. The XRD lines for the MCM-41 samples synthesized without pH adjustment in Figure 1b,d (i.e., obtained after heating the initial surfactant-silicate or aluminosilicate gel mixtures for 4 days in an oven at 370 K) are severely broadened due to a loss in the textural uniformity upon calcination of the materials. The loss of the textural uniformity has been confirmed by ¹²⁹Xe NMR line broadening.¹⁵ Lattice contractions as much as 15–25% also follow the calcination. Such large lattice contractions and severe

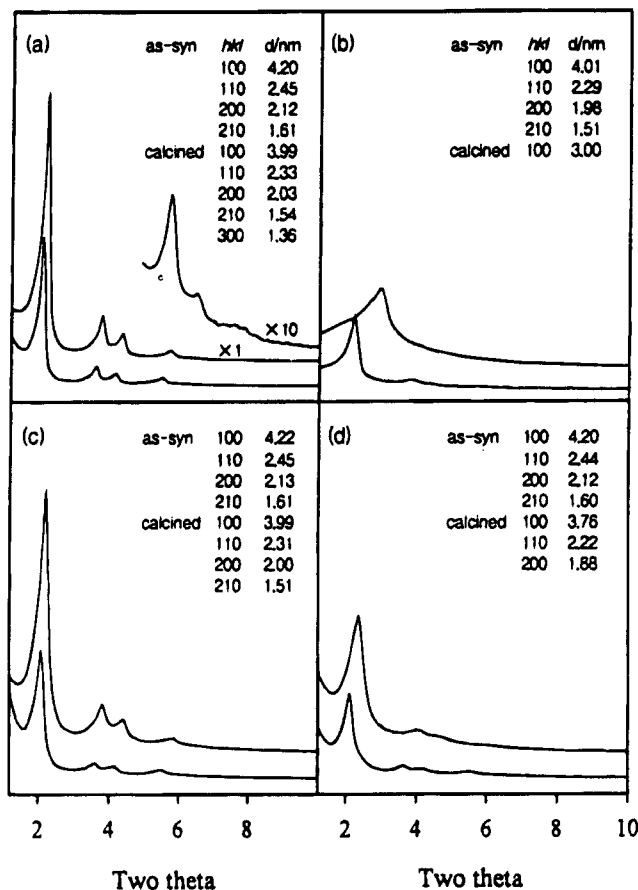


Figure 1. XRD patterns of MCM-41 samples obtained using a Cu K α X-ray source: (a) pure-silica MCM-41 synthesized following a procedure for pH adjustment to 10.2 repeated three times in all with acetic acid; (b) pure-silica MCM-41 synthesized without pH adjustment; (c) AlMCM-41 with a Si/Al ratio of 39 synthesized from a gel composition of 6 SiO₂:0.1 Al₂O₃:1 hexadecyltrimethylammonium chloride:0.25 dodecyltrimethylammonium bromide:0.25 tetrapropylammonium bromide:0.15 (NH₄)₂O:1.5 Na₂O:300 H₂O with pH adjustment; and (d) AlMCM-41 synthesized without pH adjustment. The as-synthesized samples were washed with doubly distilled water and dried in oven at 370 K. The calcination of the pure-silica MCM-41 was performed in air over 4 h at 773 K, while the calcination of the AlMCM-41 was performed over 10 h at 813 K.

XRD line broadening upon calcination of MCM-41 samples are similar to those reported previously from other laboratories.^{10,11} On the contrary, the lattice contraction for other samples synthesized by repeating pH adjustment to 10.2 three times in all is less than 5%, and the XRD line broadening is negligible. The presence of a (300) diffraction line for these MCM-41 samples indicates excellent textural uniformity after calcination. Thus, the thermal stability and textural uniformity of MCM-41 have been markedly improved by repeating the pH adjustment during hydrothermal synthesis of MCM-41. This effect can be attributed to increasing degrees of silanol group condensation in MCM-41 due to equilibrium shifts for the silicate polymerization, as proposed by Ryoo and Kim.¹⁵

Ion Exchange of AlMCM-41. Figure 2 shows MAS ²⁷Al NMR spectra of an AlMCM-41 sample used for the characterization of ion exchange property and hydrothermal stability. The sample was synthesized by repeating pH adjustment to 10.2 three times, and the Si/Al ratio was 39. The sample as-synthesized shows a ²⁷Al NMR spectrum (spectrum a) with only a tetrahedral aluminum NMR peak shifted to 50 ppm with respect to Al(H₂O)₆³⁺. The line width for the tetrahedral aluminum NMR peak after calcination at 813 K increased in spectrum b. The NMR line width decreased markedly when

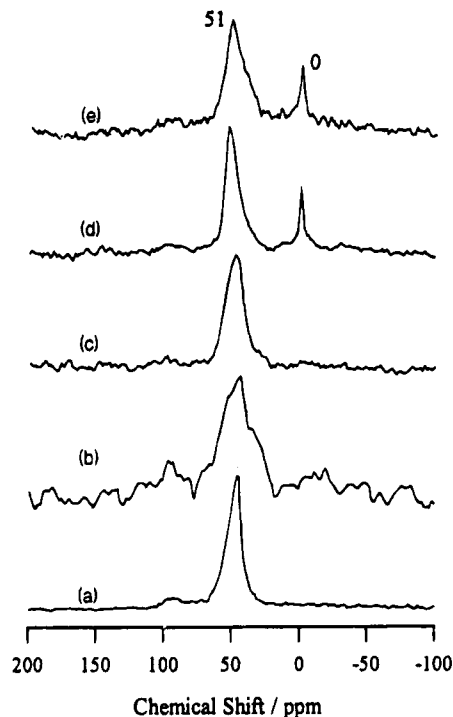


Figure 2. ²⁷Al MAS NMR spectra of AlMCM-41 samples with a Si/Al ratio of 39: (a) as-synthesized; (b) as-calcined; (c) as-calcined and then partially hydrated; (d) as-calcined and then fully hydrated; and (e) yttrium-exchanged AlMCM-41, fully hydrated after heating in the O₂ flow with 2.3 kPa of water vapor at 1170 K and fully hydration.

the calcined sample was partially hydrated, by drying at 370 K after wetting (spectrum c). However, when the sample was fully hydrated, there appeared a narrow octahedral aluminum NMR line centered approximately at 0 ppm (spectrum d). The peak area integrated under the tetrahedral aluminum peak was approximately 4 times larger than that of the octahedral peak. Thus, the presence of octahedral aluminum NMR signal for the calcined sample depended on the degree of sample hydration. The narrow octahedral peak in Figure 2d seems to come from Al(H₂O)₆³⁺ remaining as ion exchanged after dealumination from framework. Excessive line broadening due to rapid quadrupolar relaxation seems to make it difficult to detect the MAS ²⁷Al NMR signal when octahedral symmetry is distorted by loss of ligands H₂O upon dehydration. The absence of octahedral aluminum peaks in a MAS ²⁷Al NMR spectrum of AlMCM-41 does not mean that all aluminum atoms are tetrahedral. The amount of tetrahedrally coordinated framework aluminum may be better estimated from ion exchange capacity of the AlMCM-41 than the intensity of tetrahedral aluminum NMR signal.

The ion exchange of AlMCM-41 can be confirmed by reversible uptakes of sodium and potassium when the AlMCM-41 sample is subjected to "slurry-filtration-wash" cycles (*vide ante*) using NaNO₃ and KNO₃ solutions in turn. For this purpose, the following experiment has been carried out. First, the calcined AlMCM-41 sample was treated with three "slurry-filtration-wash" cycles using NaNO₃ solution. The Na content increased to 0.41 Na/Al during the treatment. Then, the sample was subjected to three more "slurry-filtration-wash" cycles using KNO₃ solution. The Na content decreased to 0.01 Na/Al during the treatment, but the K content increased to 0.36 K/Al. When the sample was further subjected to three "slurry-filtration-wash" cycles using NaNO₃ solution, the Na content and the K content changed to 0.40 Na/Al and 0.02 K/Al, respectively. These results clarify that ion exchanges of the

TABLE 1: Ion Exchange and Hydrothermal Stability of Pure-Silica MCM-41 and AlMCM-41

sample	ion ^a	ion/Al ^b	S _{BET} /m ² g ⁻¹ ^c	T _m /K ^d
pure-silica MCM-41	Na		927	980
	K			
	Ca			
	Y			
AlMCM-41 (Si/Al = 39)	Na	0.41	1016	1070
	K	0.36	984	
	Ca	0.37	982	1170
	Y	0.39	995	1170

^a Ion exchange of the MCM-41 was carried out with metal nitrate solution. ^b Elemental analysis for the metal to aluminum ratio was performed with inductively coupled plasma emission spectroscopy. Ion exchange capacity of the pure-silica MCM-41 was less than 1% compared with same mass of AlMCM-41. ^c BET area measurement was carried out with N₂ adsorption using a conventional volumetric gas adsorption apparatus. ^d T_m is defined as a maximum temperature to which MCM-41 and AlMCM-41 samples can be heated for 2 h in the O₂ flow with 2.3 kPa of water vapor, without decreasing the BET areas more than 10%.

AlMCM-41 sample with Na⁺ and K⁺ occurred reversibly, similar to the ion exchange of aluminosilicate zeolites.

The ion exchange levels in Table 1 are the metal to aluminum ratios obtained by elemental analysis after three "slurry-filtration-wash" cycles. The Na⁺ exchange level has been obtained with the AlMCM-41 sample as calcined, while the K⁺, Ca²⁺, and Y³⁺ ion exchange levels have been obtained with the AlMCM-41 sample after Na⁺ ion exchange. Assuming that the ion exchange occurs with 1 monovalent metal ion per tetrahedral aluminum site, the results with 0.41 Na/Al and 0.36 K/Al in Table 1 suggest that approximately 40% of the total aluminum atoms in the calcined AlMCM-41 are tetrahedrally coordinated within framework. However, it is not evident how the ion exchange levels for calcium and yttrium are as high as 0.37 Ca/Al and 0.39 Y/Al. It may be speculated that these ions are exchanged as hydroxymetal ions that have an overall charge of +1, or silanol groups located near the tetrahedral aluminum sites may participate in the ion exchange. At any rate, our AlMCM-41 sample has a much higher capacity for ion exchange than pure-silica MCM-41 on the same mass basis as Table 1 shows. Considering a silanol group content of pure-silica MCM-41 as high as 0.3 OH/Si after calcination,^{13,15} the silanol group in the pure-silica MCM-41 does not have a significant capacity for cation exchange under the present experimental conditions with pH = 6–7, which is similar to amorphous silica.

Figure 3 shows ¹²⁹Xe NMR spectra obtained from xenon adsorbed on ion exchanged AlMCM-41. The chemical shift of the xenon is plotted against the xenon pressure in Figure 4. The chemical shifts at the same pressure show a marked difference between samples with different cations. The difference has occurred without significant changes in the textural uniformity or the specific surface area upon the ion exchange. The XRD pattern and the BET area of the ion exchanged AlMCM-41 are shown in Figure 7.

In Figure 4, the ¹²⁹Xe NMR chemical shift for the Na⁺-exchanged AlMCM-41 is almost independent of xenon pressure changes. However, the chemical shift for the Ca²⁺-exchanged AlMCM-41 is much larger than the chemical shift for the Na⁺-exchanged AlMCM-41. Their chemical shift difference at the same pressure increases as xenon pressure decreases. The chemical shift increase for the Ca²⁺-exchanged AlMCM-41 against the pressure decrease is very similar to that for Ca²⁺-exchanged Y zeolite (CaY zeolite), which has been attributed to strong adsorption of xenon on Ca²⁺ ions located inside the supercage.^{18–20} It seems that the xenon adsorption on Ca²⁺ ions

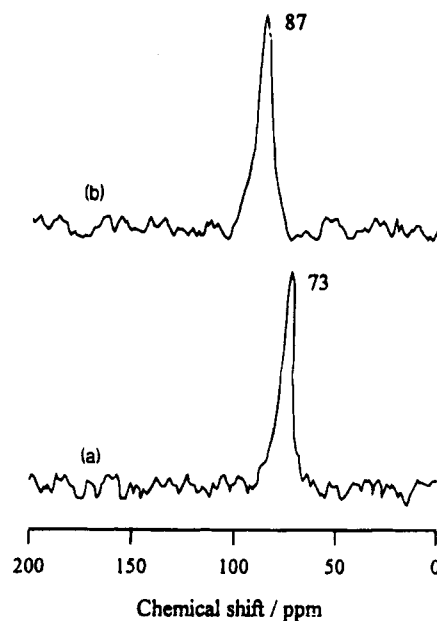


Figure 3. ¹²⁹Xe NMR spectra for ion-exchanged AlMCM-41 (Si/Al = 39) samples: (a) Na⁺-exchanged AlMCM-41 and (b) Ca²⁺-exchanged AlMCM-41. Xenon gas was equilibrated over 30 min with the sample at 296 K under 53.3 kPa. The ¹²⁹Xe NMR spectra were obtained at 296 K with a Bruker AM-300 FT NMR spectrometer operating at 83.0 MHz.

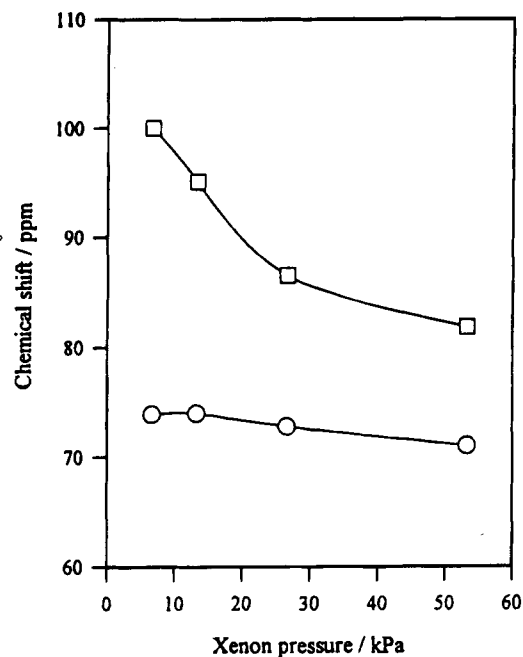


Figure 4. Chemical shift in ¹²⁹Xe NMR spectrum of adsorbed xenon on ion-exchanged AlMCM-41 (Si/Al = 39) plotted against xenon pressure at 296 K: (O) Na⁺-exchanged AlMCM-41; and (□) Ca²⁺-exchanged AlMCM-41.

in the AlMCM-41 is also strong while the adsorption on other parts of the mesopore wall is weak. Similar to CaY zeolite, the strong adsorption of xenon on Ca²⁺ seems to become saturated as xenon pressure increases above 30 kPa whereas the weak xenon adsorption increases approximately linearly with pressure according to the Henry's law. If the strong adsorption causes a much larger chemical shift than the weak adsorption as for CaY zeolite and the chemical shift is averaged due to rapid exchange of xenon between different adsorption sites, the average value will decrease as the relative population of xenon on the weak adsorption sites increases with the pressure increase.

The heat of adsorption of xenon on the AlMCM-41 with

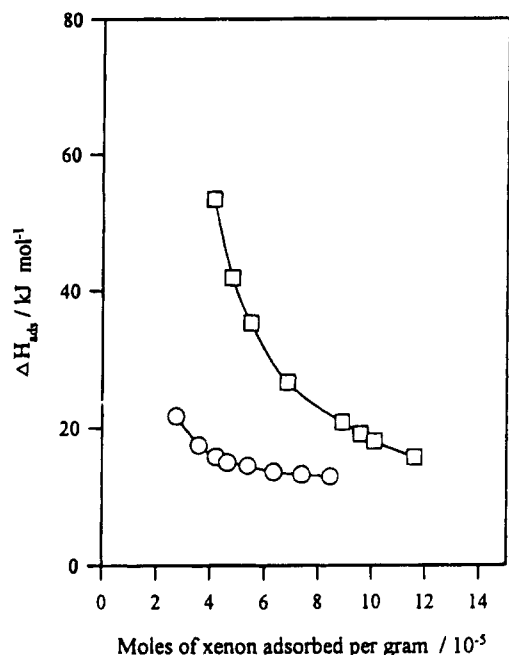


Figure 5. Heat of adsorption of xenon adsorbed on ion exchanged AIMCM-41 (Si/Al = 39) samples: (O) Na⁺-exchanged AIMCM-41; and (□) Ca²⁺-exchanged AIMCM-41.

various ion exchange has been measured at 296 K by using the Clausius-Clapeyron equation, $\Delta H_{\text{ads}}/R = -[\partial \ln P/\partial(1/T)]_m$, for the xenon adsorption isotherms obtained precisely at 293, 296, and 299 K. This ΔH_{ads} is plotted in Figure 5 as a function of the total amount of adsorbed xenon (m). The ΔH_{ads} for the Ca²⁺-exchanged AIMCM-41 shown in Figure 5 is much larger than that for the Na⁺-exchanged AIMCM-41. At 6.7 kPa, the ΔH_{ads} for the Ca²⁺-exchanged AIMCM-41 is as large as -50 kJ mol^{-1} . However, the magnitude of ΔH_{ads} decreases with the increase of m , approaching to an almost constant value of -15 kJ mol^{-1} , which equals to ΔH_{ads} for the Na⁺-exchanged sample. This result confirms strong adsorption of xenon on Ca²⁺ inside the AIMCM-41 channel.

Thermal Stability and Hydrothermal Stability of MCM-41. Figures 6 and 7 display changes in XRD pattern and BET area when calcined pure-silica MCM-41 and AIMCM-41 (Si/Al = 39) samples were heated at various temperatures. The sample heating was carried out for 2 h at each temperature in flows (at $2 \text{ L min}^{-1} \text{ g}^{-1}$) of dry O₂ and O₂ with 2.3 kPa of water vapor. The XRD patterns were obtained under same experimental conditions after cooling all the samples to room temperature. The XRD intensities in Figures 6 and 7 are directly comparable to each other since the values are plotted using the same scale. Both the XRD intensity and the BET area show similar decreasing tendencies with increase of the heating temperature. Therefore, both XRD intensity and BET area may equally be used to probe thermal stability of MCM-41 samples.

The XRD patterns for the pure-silica MCM-41 in Figure 6 show that the XRD lines broadened gradually as the heating temperature increased to 1143 K in dry O₂. Although the XRD patterns show somewhat decreasing in the d_{100} spacing, the magnitude of the lattice size contraction is still much less than those reported by Chen et al.¹⁰ The height of the (100) XRD line after the heating at 1073 K does not show a considerable decrease, compared with the as-calcined sample. Decreases in the BET area of the sample is still less than 10% even after heating at 1143 K. Thus, it may be stated that the thermal stability of the pure-silica MCM-41 material extends to 1143

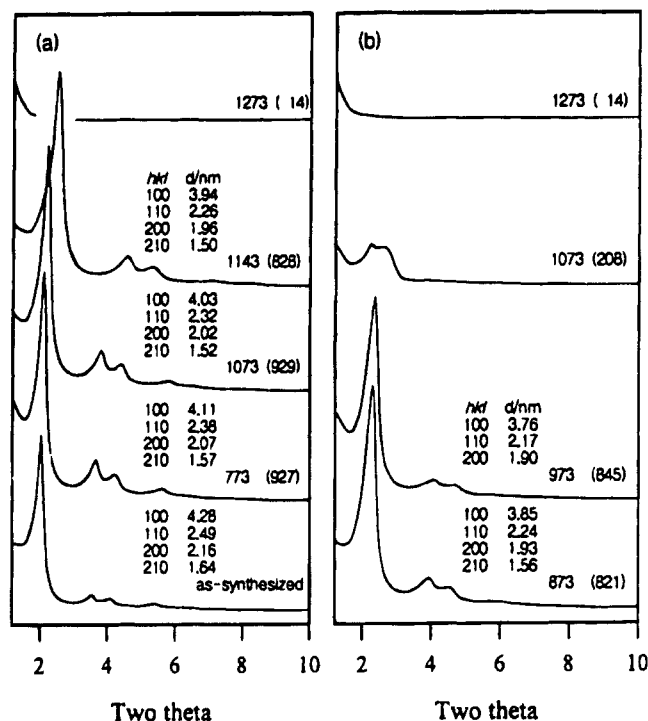


Figure 6. XRD patterns of pure silica MCM-41 samples after thermal and hydrothermal treatment: (a) thermal treatment in dry O₂ flow and (b) hydrothermal treatment in O₂ flow saturated with water vapor at room temperature. Calcined pure-silica MCM-41 samples were heated through O₂ flow in a quartz U-tube reactor for 2 h at each temperature. Numbers before parentheses indicate the heating temperature in kelvin, and the numbers in the parentheses denote BET areas ($\text{m}^2 \text{ g}^{-1}$) of the samples after heating.

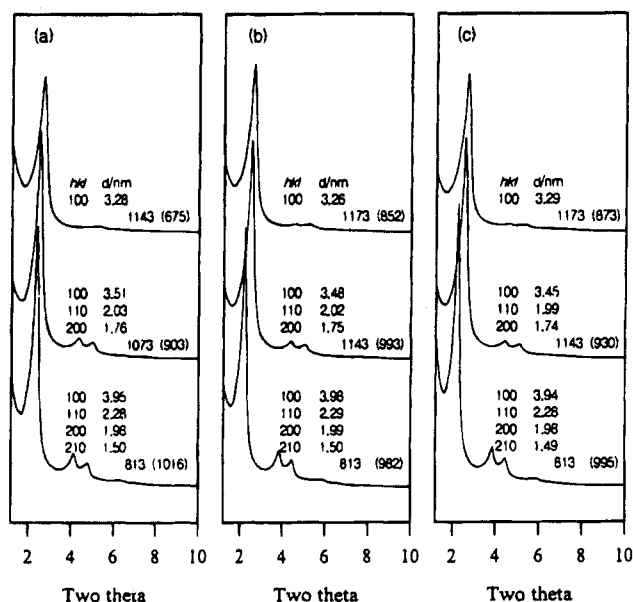


Figure 7. XRD patterns of ion-exchanged AIMCM-41 (Si/Al = 39) samples after hydrothermal treatment: (a) Na⁺-exchanged AIMCM-41; (b) Ca²⁺-exchanged AIMCM-41; and (c) yttrium-exchanged AIMCM-41. Numbers before parentheses indicate the heating temperature in kelvin, and the numbers in the parentheses denote BET areas ($\text{m}^2 \text{ g}^{-1}$) of the samples after heating.

K in dry O₂. Similarly, the hydrothermal stability of the sample in the O₂ with 2.3 kPa of water vapor can be stated to extend to 980 K.

In Table 1, T_m is defined as a maximum temperature to which AIMCM-41 samples can be heated for 2 h in the O₂ flow with 2.3 kPa of water vapor, without decreasing the BET areas more than 10%. Figure 7 and Table 1 show that T_m is affected by

the ion exchange as follows: Y^{3+} (1170 K) \sim Ca^{2+} $>$ Na^+ (1070 K) \sim as-calcined AlMCM-41 $>$ pure-silica MCM-41 (980 K). Thus, the AlMCM-41 samples show excellent hydrothermal stability particularly after the ion exchange with Ca^{2+} and yttrium. As shown in Figure 2e, MAS ^{27}Al NMR spectra obtained after heating in the O_2 flow with 2.3 kPa of water vapor at T_m still shows a tetrahedral aluminum NMR peak centered at 50 ppm with a signal intensity 4 times greater than the octahedral aluminum NMR peak.

Conclusion

In the present investigation, AlMCM-41 with a Si/Al ratio of 39 exhibited ion exchange capacities up to 0.41 Na/Al, 0.36 K/Al, 0.37 Ca/Al, and 0.39 Y/Al. On the contrary, pure-silica MCM-41 showed no significant levels of the ion exchange. The ion exchange in AlMCM-41 occurred onto framework aluminum sites. The ion-exchanged AlMCM-41 showed a remarkable thermal stability when heated in O_2 flow saturated with water vapor at room temperature, for 2 h at various temperatures. The maximum temperatures, at which the BET areas decreased less than 10%, depended on the cation exchange as follows: Y^{3+} (1170 K) \approx Ca^{2+} $>$ Na^+ (1070 K) \approx as-calcined AlMCM-41 $>$ pure-silica MCM-41 (980 K). High ion exchange capacity and good thermal stability of MCM-41 suggest that the material can be used for such applications as requiring metal ion exchange and high-temperature stability.

References and Notes

- (1) Kresge, C. T.; Leonowicz, M. E.; Roth, W. J.; Vartuli, J. C.; Beck, J. S. *Nature* **1992**, *359*, 710.
- (2) Beck, J. S.; Vartuli, J. C.; Roth, W. J.; Leonowicz, M. E.; Kresge, C. T.; Schmitt, K. D.; Chu, C. T.-W.; Olson, D. H.; Sheppard, E. W.; McCullen, S. B.; Higgins, J. B.; Schlenker, J. L. *J. Am. Chem. Soc.* **1992**, *114*, 10834.
- (3) (a) Corma, A.; Navarro, M. T.; Pérez-Pariente, J. *J. Chem. Soc., Chem. Commun.* **1994**, 147. (b) Corma, A.; Navarro, M. T.; Pérez-Pariente, J.; Sánchez, F. In *Zeolites and Related Materials: State of the Art 1994*; Weitkamp, J., et al., Eds.; Studies in Surface Science and Catalysis, Vol.

- 84; Elsevier: Amsterdam, 1994; pp 69–75.
- (4) Tanev, P. T.; Chibwe, M.; Pinnavaia, T. J. *Nature* **1994**, *368*, 321.
- (5) Reddy, K. M.; Moudrakovski, I.; Sayari, A. *J. Chem. Soc., Chem. Commun.* **1994**, 1059.
- (6) (a) Wu, C.-G.; Bein, T. *Science* **1994**, *264*, 1757. (b) Wu, C.-G.; Bein, T. In *Zeolites and Related Materials: State of the Art 1994*; Weitkamp, J., et al., Eds.; Studies in Surface Science and Catalysis, Vol. 84; Elsevier: Amsterdam, 1994; pp 2269–2276.
- (7) Llewellyn, P. L.; Ciesla, U.; Decher, H.; Stadler, R.; Schüth, F.; Unger, K. K. In *Zeolites and Related Materials: State of the Art 1994*; Weitkamp, J., et al., Eds.; Studies in Surface Science and Catalysis, Vol. 84; Elsevier: Amsterdam, 1994; pp 2013–2020.
- (8) Monnier, A.; Schüth, F.; Huo, Q.; Kumar, D.; Margolese, D.; Maxwell, R. S.; Stucky, G. D.; Krishnamurty, M.; Petroff, P.; Firouzi, A.; Janicke, M.; Chmelka, B. F. *Science* **1993**, *261*, 1299.
- (9) Huo, Q.; Margolese, D. I.; Ciesla, U.; Feng, P.; Gier, T. E.; Sieger, P.; Leon, R.; Petroff, P. M.; Schüth, F.; Stucky, G. *Nature* **1994**, *368*, 317.
- (10) (a) Chen, C.-Y.; Li, H.-X.; Davis, M. E. *Microporous Mater.* **1993**, *2*, 17. (b) Chen, C.-Y.; Burkett, S. L.; Li, H.-X.; Davis, M. E. *Microporous Mater.* **1993**, *2*, 27. (c) Chen, C.-Y.; Xiao, S.-Q.; Davis, M. E. *Microporous Mater.* **1995**, *4*, 1.
- (11) Janicke, M.; Kumar, D.; Stucky, G. D.; Chmelka, B. F. In *Zeolites and Related Materials: State of the Art 1994*; Weitkamp, J., et al., Eds.; Studies in Surface Science and Catalysis, Vol. 84; Elsevier: Amsterdam, 1994; pp 243–250.
- (12) (a) Schmidt, R.; Akporiaye, D.; Stöcker, M.; Ellestad, O. H. *J. Chem. Soc., Chem. Commun.* **1994**, 1493. (b) Schmidt, R.; Akporiaye, D.; Stöcker, M.; Ellestad, O. H. In *Zeolites and Related Materials: State of the Art 1994*; Weitkamp, J., et al., Eds.; Studies in Surface Science and Catalysis, Vol. 84; Elsevier: Amsterdam, 1994; pp 61–68.
- (13) Kolodziejski, W.; Corma, A.; Navarro, M.-T.; Pérez-Pariente, J. *Solid State Nucl. Magn. Reson.* **1993**, *2*, 253.
- (14) Corma, A.; Fornés, V.; Navarro, M. T.; Pérez-Pariente, J. *J. Catal.* **1994**, *148*, 569.
- (15) Ryoo, R.; Kim, J. M. *J. Chem. Soc., Chem. Commun.* **1995**, 711.
- (16) XRD patterns show that the structure of AlMCM-41 can be readily destroyed during Na^+ ion exchange when the exchange level is high. The details are being investigated.
- (17) Feuton, B. P.; Higgins, J. B. *J. Phys. Chem.* **1994**, *98*, 4459.
- (18) Pak, C.; Ryoo, R. *J. Korean Chem. Soc.* **1992**, *36*, 351.
- (19) Ito, T.; Fraissard, J. *J. Chem. Soc., Faraday Trans. 1* **1987**, *83*, 451.
- (20) Kim, J.-G.; Kompany, T.; Ryoo, R.; Ito, T.; Fraissard, J. *Zeolites* **1994**, *14*, 427.